CHAPTER 31

VELOCITIES UNDER PERIODIC AND RANDOM WAVES

by

Allen Lee

Research Student, Fluid Dynamics Unit , Edinburgh University

Clive A. Greated

Director, Fluid Dynamics Unit, Edinburgh University

and

Tariq S. Durrani

Research Fellow, Electronics Dept., Southampton University

ABSTRACT

Using the linear approximation for predicting velocities under periodic water waves, relationships are established between the velocity spectrum and the surface elevation spectrum for three-dimensional waves. The two dimensional forms of these relationships are used for comparison with velocity and elevation spectra measured in a laboratory wave tank. The predicted distortion of the spectrum shape can be observed in the experimental results. Velocity measurements were recorded using a laser velocimeter employing a rotating diffraction grating for shifting the optical frequencies. This allows measurement without sign ambiguity. The random waves were generated using a servo-driven paddle with a filtered white noise input.

INTRODUCTION

One of the main problems in coastal engineering is to determine the velocity distribution beneath ocean waves; for the purpose of predicting wave forces on structures and sediment transport behaviour etc. Direct measurements in the ocean are difficult because of the violent action in the waves of most interest. Data interpretation is also difficult, due to the distortion in the results given by conventional velocity meters. There is, however, a range of methods in wide use, for measuring surface elevation spectra and surface probability distributions. Hence if a generally valid relationship between surface statistics and under-surface velocity statistics for waves can be established, the problem of accurately predicting wave force distributions reduces to that of applying a transformation to measured surface statistics.

The search for such a relationship is well suited as a laboratory research problem, particularly with the increasing availability of random wave generating machines. Reliable wave height gauges are also in common use. Until recently the velocities under the waves were still measured with ultrasonic meters or rotating vane meters, with the consequent interference to the flow. In this paper we show that the velocities can be measured without disturbing the flow, if the laser doppler velocimeter technique (referred to as L.D.V.) is used. The method is explained and our laboratory apparatus, with the L.D.V., is described. We are using this system to examine the link between water surface position and the velocities beneath the surface for random waves. The results given here are drawn from the experiments we did to see the limitations of the linear wave theory. Comparisons are made between measured velocity spectra and those obtained by 'linearly' transforming surface elevation spectra.

THE LINEAR WAVE EQUATIONS

Using the linearized potential flow equations, i.e. neglecting second order terms in the equations of motion, the potential under a periodic wave of surface profile

$$\eta\ (x,t) = a \cos\ (\mu x - \omega t)$$

is

$$\Phi\ (x,z,t) = \frac{ga}{\omega}\ \frac{\cosh \mu\ (z + h)}{\cosh \mu h} \sin\ (\mu x - \omega t) \qquad (1)$$

where μ is the wave number, ω the frequency, z the position above still water level and h the water depth. The wave number and frequency are related by the equation

$$\omega^2 = g\mu \tanh\ (\mu h) \qquad (2)$$

The concept of a velocity potential can be extended to three-dimensional seas.

Consider the random surface defined at any point (x,y) to be

$$\eta\ (x,y,t) = \sum_i C_i \cos\ (\mu_i x + \nu_i y - \omega_i t - \epsilon_i) \qquad (3)$$

where $\{C_i\}$ are Gaussian distributed variables representing the random amplitudes of the stochastic surface; $\{\mu_i, \nu_i\}$ are now wave numbers in the x and y directions respectively; $\{\omega_i\}$ are the component frequencies and $\{\epsilon_i\}$ the random phases. According to the linear approximation the stochastic potential is now given by

$$\Phi(x,y,z,t) = g\sum_i \frac{C_i}{\omega_i} \frac{\cosh\left\{\sqrt{\mu_i^2 + \nu_i^2}\,.\,(z+h)\right\}}{\cosh\left\{\sqrt{\mu_i^2 + \nu_i^2}\,.h\right\}} \sin\left\{\mu_i x + \nu_i y - \omega_i t - \epsilon_i\right\} \tag{4}$$

Defining $\mu_i = k_i \cos\theta_i$ and $\nu_i = k_i \sin\theta_i$ the frequency spectrum of the surface elevation is related to the three-dimensional spectrum by

$$\Phi(\omega) = \int_0^\infty \int_0^{2\pi} k\,\Phi(k,\theta,\omega)\,dk\,d\theta \tag{5}$$

The instanteous frequencies and wave numbers are related by

$$\omega_i^2 = g\,k_i \tanh k_i h \tag{6}$$

From equation (4) the instantaneous velocities at vertical position z in the x and y directions respectively are

$$U_x = \frac{\partial\Phi}{\partial x} = g\sum_i \frac{C_i\mu_i}{\omega_i} \frac{\cosh k_i (z+h)}{\cosh k_i h} \cos(\mu_i x + \nu_i y - \omega_i t - \epsilon_i) \tag{7}$$

and

$$U_y = \frac{\partial\Phi}{\partial y} = g\sum_i \frac{C_i\nu_i}{\omega_i} \frac{\cosh k_i (z+h)}{\cosh k_i h} \cos(\mu_i x + \nu_i y - \omega_i t - \epsilon_i) \tag{8}$$

In a laboratory channel with no motion in the y direction then equation (7) holds with $\nu_i = 0$ so the relationship between the surface elevation spectrum $\Phi(\omega)$ and the horizontal velocity spectrum $\psi(\omega)$ is

$$\psi(\omega) = \omega^2 \frac{\cosh^2 k(z+h)}{\sinh^2(kh)} \Phi(\omega) \tag{9}$$

In writing equation (9) the dispersion relationship of equation (6) has been introduced. Equation (9) is the formula that gives the transformation from the elevation to velocity spectrum in the two-dimensional laboratory situation. This theoretical transformation is to be compared with experiment.

Starting from equations (7) and (8) one can also compute statistics which are applicable to the three-dimensional situation. For example, we find that the expected value of the instantaneous horizontal velocity **in deep water is**

$$E\,[U_x^2 + U_y^2] = \tfrac{1}{2}\sum_i E\,[\omega_i^2\,C_i^2\,e^{2.\frac{\omega_i^2 z}{g}}]$$

i.e. an exponential decay with depth. As yet though, we have no means of comparing theory with experiment in a three-dimensional sea.

THE LASER DOPPLER VELOCIMETER

The laser doppler system for measuring particle velocities is not well known to experimenters interested in waves. We intend to show that the instrument is both simple to set up and convenient to use. Its accuracy is well documented in the journals (Durrani and Greated, 1973 and 1974).

Essentially the method depends on Doppler's principle that relative motion between a source of radiation and an observer produces a change in the frequency of the observed radiation. Although there are many optical arrangements, the twin beam system is the most common. In this a laser beam is wavefront or amplitude divided into two separated and coherent parallel beams. A lens is used to focus these into the flow, where the resulting optical fringe pattern is produced. Microscopic particles, which exist in and characterise most flows, will scatter light from this fringe pattern in a predominantly forward direction. If the scattered light is collected over a large solid angle and directed onto a photomultiplier or photo-diode, an electrical signal is produced by the intensity fluctuations on the detector surface. These fluctuations are directly due to particles crossing the fringes at a frequency f_D which is related to their velocity V by the formula

$$f_D = \frac{V}{d}, \text{ where } d = \frac{\lambda}{2 \sin \Phi/2} = \text{Fringe spacing}$$

(Φ is the beam crossing angle as the light enters the flow). If the light is collected over a small solid angle the scattered components of the two beams will heterodyne on the detector surface, again to produce a signal at frequency f_D (component frequencies $\{f_L + (f_D/2)\}$, $\{f_L - (f_D/2)\}$). The velocity v is the component at right-angles to the laser beams bisector. If it had the value -v, the detector would still only register the fringe crossing or shifted frequency as f_D positive. This means that in all reversing flows such as waves, the velocity sign information is normally lost. The usual solution is to give a steady offset frequency f_S to the laser frequency f_L of one of the beams. The scattered light is then

$$\left(f_L + \frac{f_D}{2} + f_S\right) \quad \text{and} \quad \left(f_L - \frac{f_D}{2}\right)$$

with a resulting detected signal of $\left(f_S + f_D\right)$. The effect is merely that of adding a D.C. offset to an electrical A.C. signal. Three methods of producing this offset will be discussed.

(a) The Circular Diffraction Grating.

The grating is rotated in the plane perpendicular to the laser output, at a constant frequency of N Hz. Then for K line pairs on the grating there will be a frequency difference between the +1 and -1 diffraction orders of N x K. The grating line pairs act as moving sources and give a conventional Doppler shift. The other grating method is to image the line pairs into the flow instead of forming a two beam fringe pattern. The image spacing is then given by the law of optical imaging and the grating movement is given to the image to produce the required offset.

(b) Acoustic Bragg Cell

This is a well known device whereby an ultrasonic wave train is directed across the laser beam path. When the two are inclined at precisely the Bragg angle for the medium, (in the plane of the ultrasonic wave direction and the beam) then the cell will act as a blazed phase grating and shift most of the laser energy into one of the first diffraction orders, with a frequency shift equal to the ultrasonic frequency, i.e. of the order ten or a hundred mega-Hertz. A second cell operated at a slightly different ultrasonic frequency is used on the second beam so the resulting difference remains in the 100 kHz range.

(c) Phase Modulators

These devices use crystals which will, upon applying a sawtooth voltage across them, give an effect such as Pockels phase modulation to a beam of light passing through the crystal. When combined with the second beam a phase modulation in the fringe pattern, and hence in the scattered light, is produced, giving the required offset at a frequency related to that of the sawtooth voltage used. Its chief advantage is that it only needs a few hundred volts D.C. to operate whereas most electro-optic devices need several thousand volts A.C. for efficient use.

Once the electrical signal (with its frequency fluctuations proportional to the particle velocities) is obtained from the detector it is most conveniently converted to an amplitude fluctuation by a frequency tracking device with phase locked feedback and fast response. The output is then directly proportional to the wave particle velocity and may be recorded for later analysis.

EXPERIMENTAL APPARATUS

Our work has been carried out on an open channel 5 m. long 30 cm. deep and 30 cm. wide. It is connected to large storage tanks and the water level can be raised or lowered by the use of a pump, as required. In our initial work we used a simple flap paddle to generate periodic waves with a synchronous electric motor providing the drive. For our work with random waves a mechanical wave generator, as indicated on figure 2, was used. It is not hydraulic in its operation and is extremely light compared to such devices. Its motion comes from an oscillating electric motor which is capable of responding to a random signal. There is almost no mechanical inertia so this is provided electronically by varying the mean position of the oscillating motor armature to give whatever trim is required. The paddle is cylindrical at the back and thus produces no backwave. The signal imput is obtained at present by bandpass filtering of white noise produced by an analogue device.

The wave heights are followed using a resistance type gauge with platinum wire elements. It is driven by a low frequency oscillator (200 Hz) and the resulting output signal is rectified and smoothed before recording. Both a flat beach and a curved beach with wire mesh covering have been used.

They have reflection co-efficients of about 6% and 3% respectively.

The L.D.V. was set up on two parallel vertical optical benches, on a rig shown in figure 3. This configuration enabled the velocities to be scanned in depth by merely sliding the prism and lens to a different position on the bench, and moving the detector correspondingly. We took special care to ensure that no part of the rig was in contact with the channel, and any floor vibration was damped by the rubber supporting pads under the steel rig.

Early on in the project we decided to use a rotating diffraction grating to eliminate the sign ambiguity of the L.D.V. The device is an 8 cm. glass disc with 3600 radial lines of chromium, driven by a 50 cycle synchronous electric motor via a 2 : 1 step-down brass gearing. This acts as a fly-wheel and gives excellent stability. For use with a 5 mW He-Ne laser we chose the method of imaging the grating into the flow. The arrangement gave adequate intensities of signal which we detected with a photo-diode device.

The signal processing for the periodic waves consisted only of a storage oscilloscope and a manual wave analyser. For the random waves the signals from the frequency tracker and the wave-height gauge we recorded simultaneously on two channels of an F.M. tape recorder. These signals were later processed by analogue methods. A spectrum analyser with automatic graph plotter was used over the range 0.3 Hz to 5 Hz and gave the energy spectra directly, with suitable scaling factors for the axes. A digital correlator was used to obtain probability density curves, autocorrelation curves and cross correlation curves, with the displays being outputted to an X-Y plotter.

RESULTS FROM PERIODIC WAVES

For the case of periodic waves, if the experimenter is satisfied that the waves are stable, there is no need for a complex analysing system. Once the waveheight, wavelength and frequency have been measured using, for instance, only an oscilloscope and a pair of battery powered bare-wire probes, then the L.D.V. signal may be scanned manually with a wave analyser. When the L.D.V. frequency signal is at that of the analyser a pulse will be produced. For periodic waves there will be a train of pulses which can be displayed on the oscilloscope and their separation in time noted. Thus a chart can be built up giving frequency change against time, i.e. particle velocity against time, as in figure 4(a). We have used this method on several occasions and have found it extremely good at recording small variations in the velocity-time trace (figure 4b). Also we have used the method to build up the velocity depth profiles in figure 5, measuring from the channel bed up to the inside of the wave crests. The variation of velocity with time in figure 4b is for a sinusoidal wave of period 0.41 s. and crest to trough height 1.73 cm. Since the water depth was 24 cm. and the wavelength 31.6 cm. we considered this to be a deep water wave. The velocity trace shown is believed to consist of the main wave plus a harmonic at 5 times the basic frequency and about one tenth the main wave amplitude. This could be due to either a reflection interacting with the paddle, or some underflow from the beach. The most interesting parts of the trace are the incomplete parts which were recorded above the trough level. The highest velocity was recorded well above the mean surface at 24.5 cm. i.e. only a few mm. under the crest maximum. The velocity value at the crest is several times that recorded at 15 cm. depth (lowest trace).

For a set wave the velocity was usually measured at depth intervals of 2 cm. and a wave cycle in figure 4b is typically constructed from about 50 points.

The depth profiles for the above wave and a similar wave in a depth of 15 cm. are shown in figure 5. The dashed profiles were calculated from the linearized wave equation, and the agreement is good for the deep water wave.

RESULTS FOR RANDOM WAVES

For three different input spectra, we have measured, from the wave gauge, the surface elevation spectra and, from the L.D.V., the velocity spectra. For a water depth of 21.75 cm. the signals were recorded for positions above the channel bed of 0.8 cm., 8.4 cm. and 16.6 cm. The amplitude probability densities of these signals are shown in Figure 6. Those for the 3 surface elevation signals are almost identical whereas the velocity density narrows considerably with depth. This amplitude fall-off is expected and we intend to study in detail the R.M.S. velocity amplitude profile with depth, at a later date. It is well known that water surface elevations for random waves are assumed to have an approximately Gaussian probability density. The elevation densities and the velocity densities all show some deviation from Gaussianity but they serve to confirm the assumption.

The measurements were made in a water depth of only 21.75 cm. with the water bed frequently disturbed during the passage of wave trains. So it was decided that the dispersion curve should be calculated in full for the determination of wave number. The curve is shown in fig. 7, with the usual deep water and shallow water approximations as dashed lines. The wave numbers were then used to compute the transformation function in equation 9.

The measured spectra are shown in figs. 8, 9 and 10, part A being the surface elevation and part B the velocity spectrum in each case. Part A also shows the transfer function over the relevant frequency range. The velocity spectra predicted by equation 9 are shown superimposed on the measured spectra, for simple comparison. The predicted effect is to shift the energy to lower frequencies with enhancement of low frequency peaks. This is clearly confirmed experimentally and in several cases the peaks in the surface spectra may be identified in the velocity spectra, with considerable change in their energy content.

Autocorrelation and cross-correlation functions have been obtained from the random wave data, however, they are of quite a complicated form and are consequently difficult to interpret. We are hoping to achieve success with the correlation analysis, in the near future.

CONCLUSIONS

The laser doppler velocimeter has been shown to be highly suitable for the laboratory study of periodic and random water waves. The initial results of a project studying the relationship between wave elevations and particle velocity fluctuations show that the system described is practical and versatile. The results for periodic waves, with the data from inside the wave crests, indicate the shortcomings of the linearized wave equation near the water surface. Further study in this upper region promises to be of great interest. The spectral results, while confirming the general value of linear wave theory, show that the inclusion of non-linear terms in the theory will be necessary if accurate wave particle velocity spectra are to be predicted.

REFERENCES

T.S. Durrani and C. Greated, 1973 'Statistical analysis and computer simulation of laser Doppler velocimeter systems', Trans. IEEE, Vol. IM 22, No. 1, pp.23-34.

T.S. Durrani and C. Greated, 1974 'Theory of L.D.V. Tracking systems', Trans. IEEE, Vol. AES. 10, No. 4, pp. 418-428.

Fig. 1 L.D.V. SYSTEMS

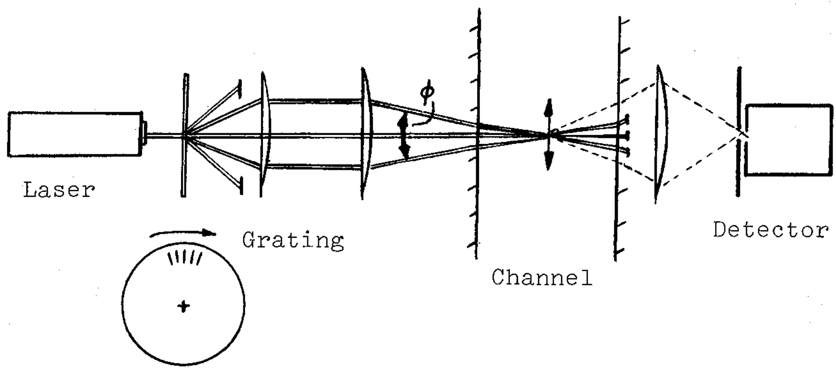

(a) With diffraction grating imaged in the flow

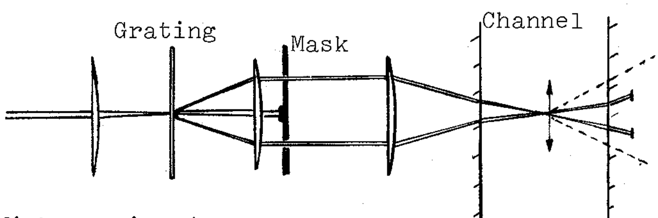

(b) With grating ±1 orders only

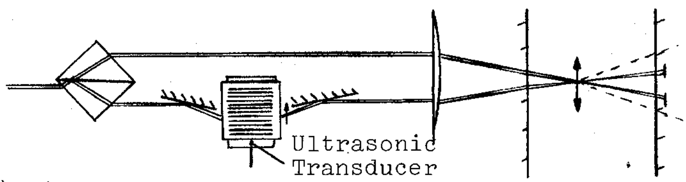

(c) With Bragg Cell

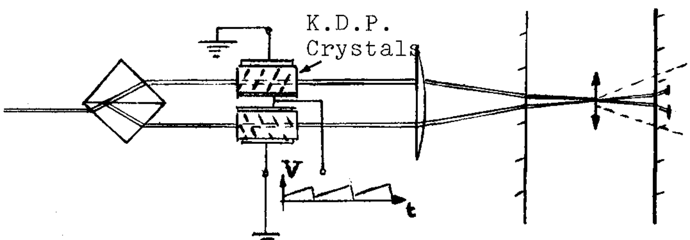

(d) With Phase modulators

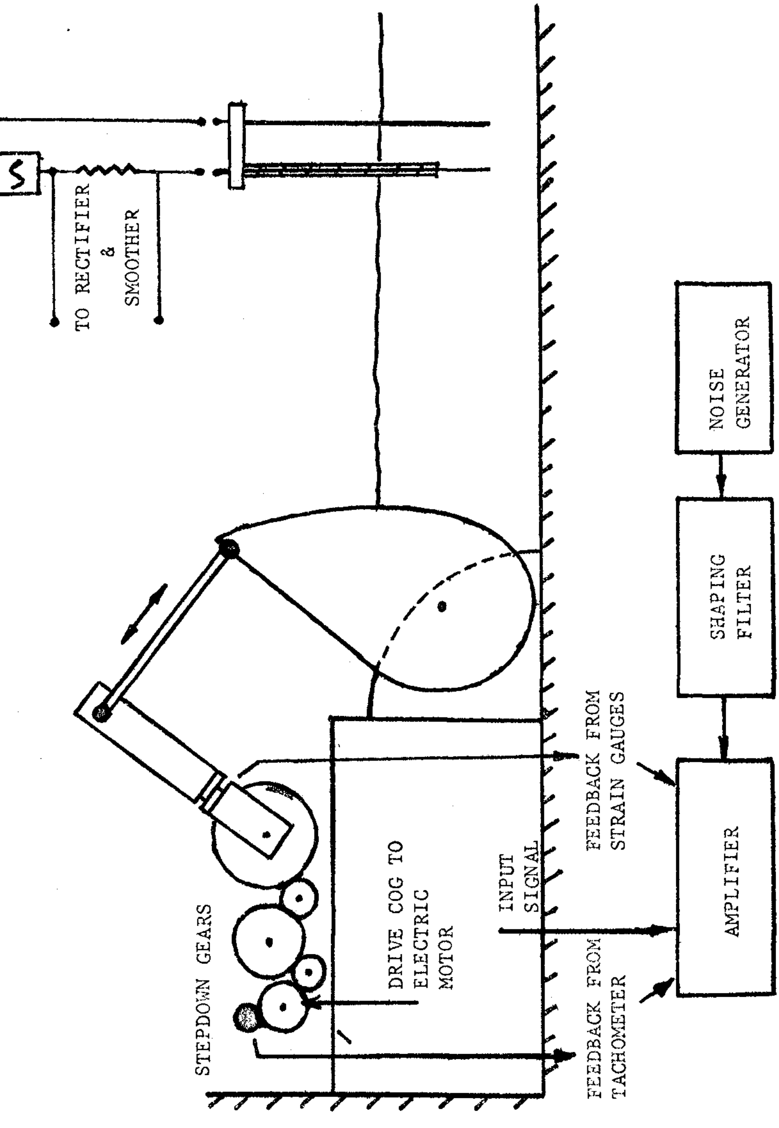

Fig. 2 RANDOM WAVE GENERATOR

WAVE HEIGHT GAUGE

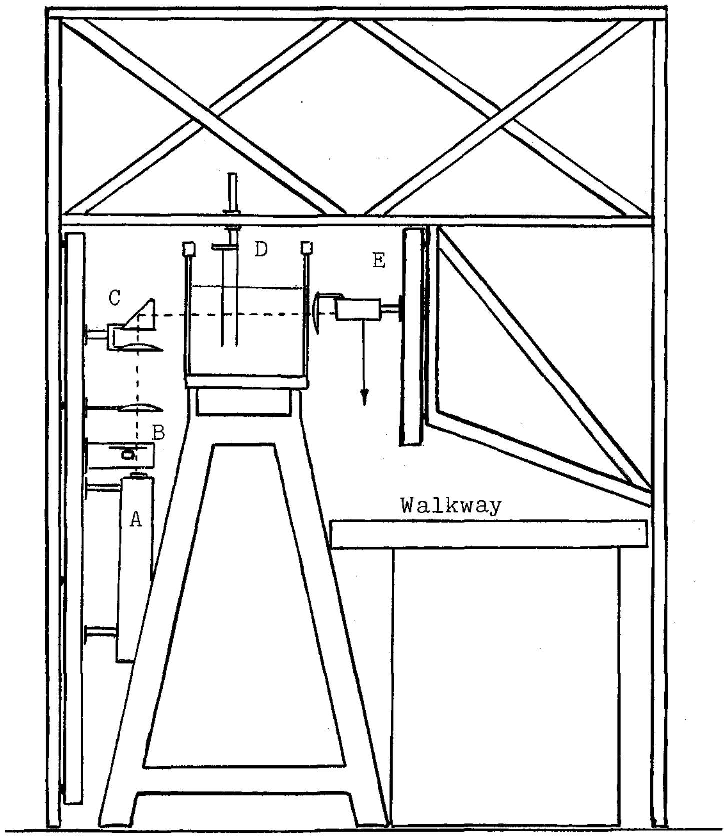

Fig. 3 L.D.V. and support Rig

A - Laser
B - Rotating Grating
C - Right angle prism
D - wave height gauge
E - detector (photo-diode)

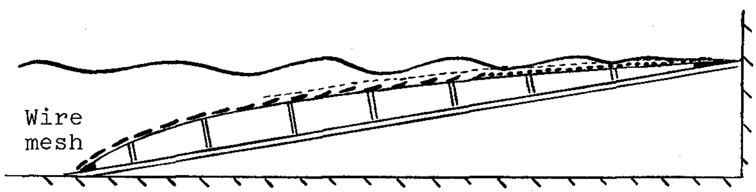

Wave Tank Beach

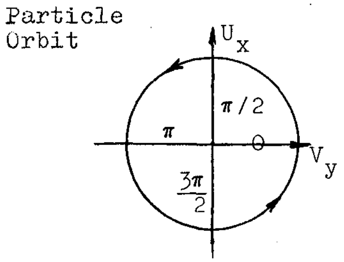

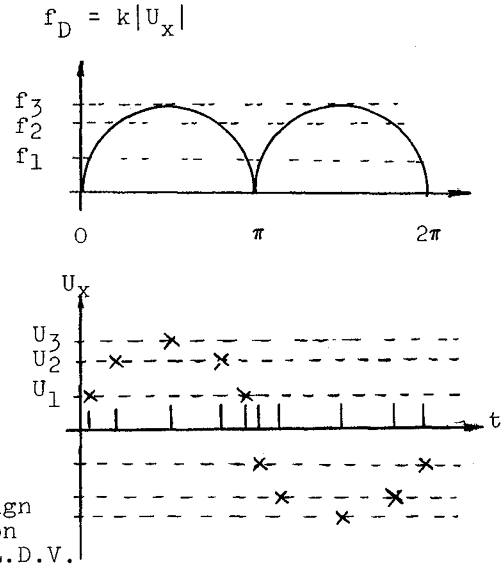

Fig. 4a
For each setting of frequency f_D the wave analyser gives a pulse train.
The occurrence of a velocity component is thus verified. Its sign is fixed by observation of crest passing the L.D.V.

Fig. 4b Velocity trace-deep water wave

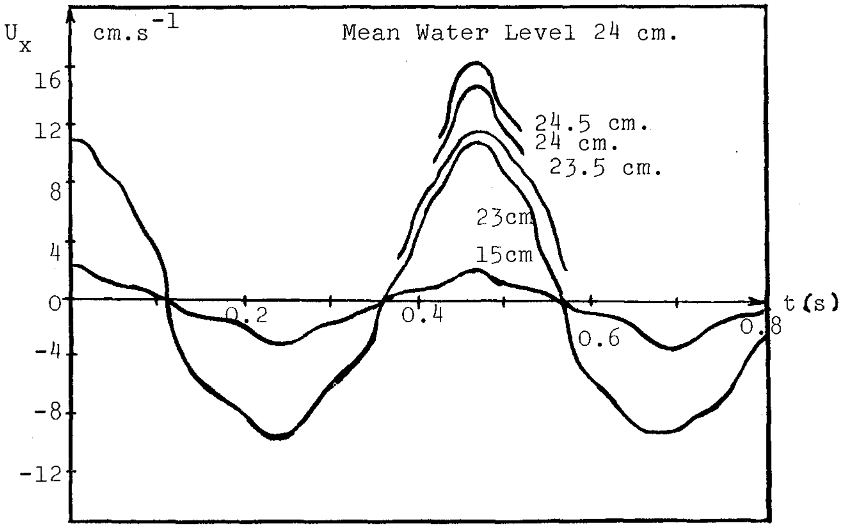

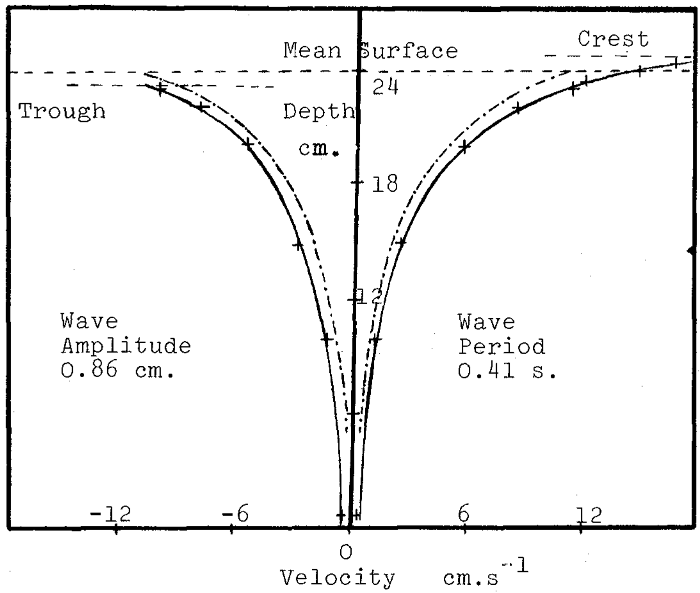

Fig. 5 Velocity-depth Profiles

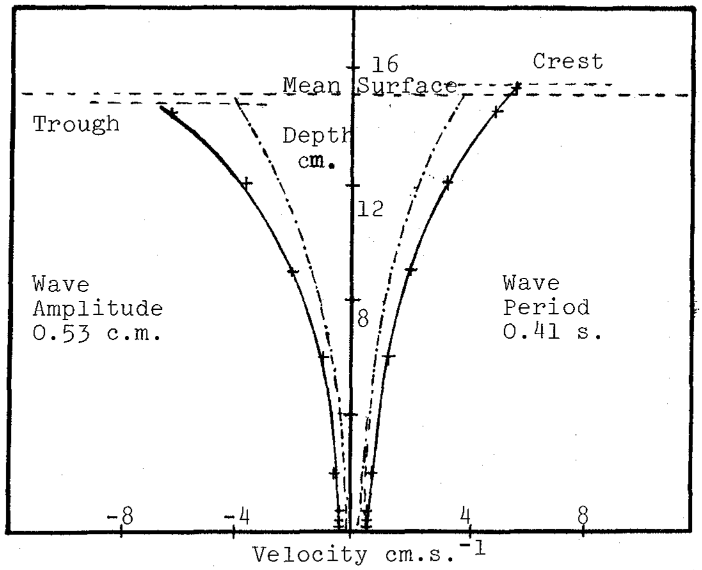

Fig. 6.

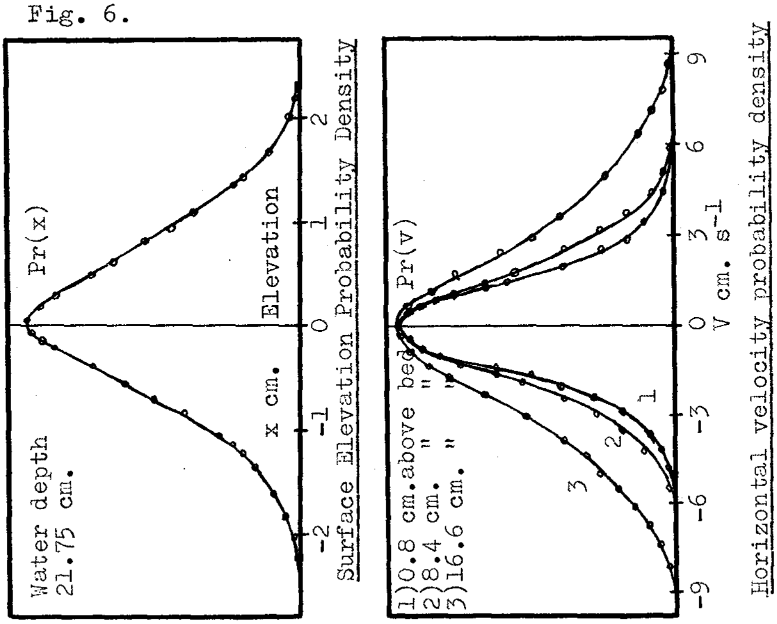

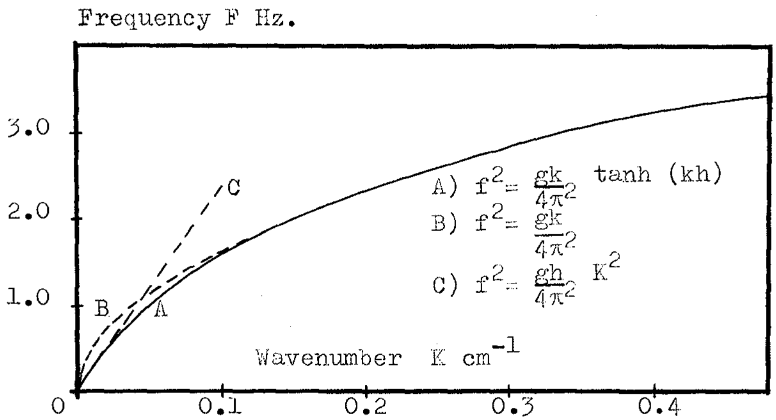

Fig. 7 Dispersion Relationship

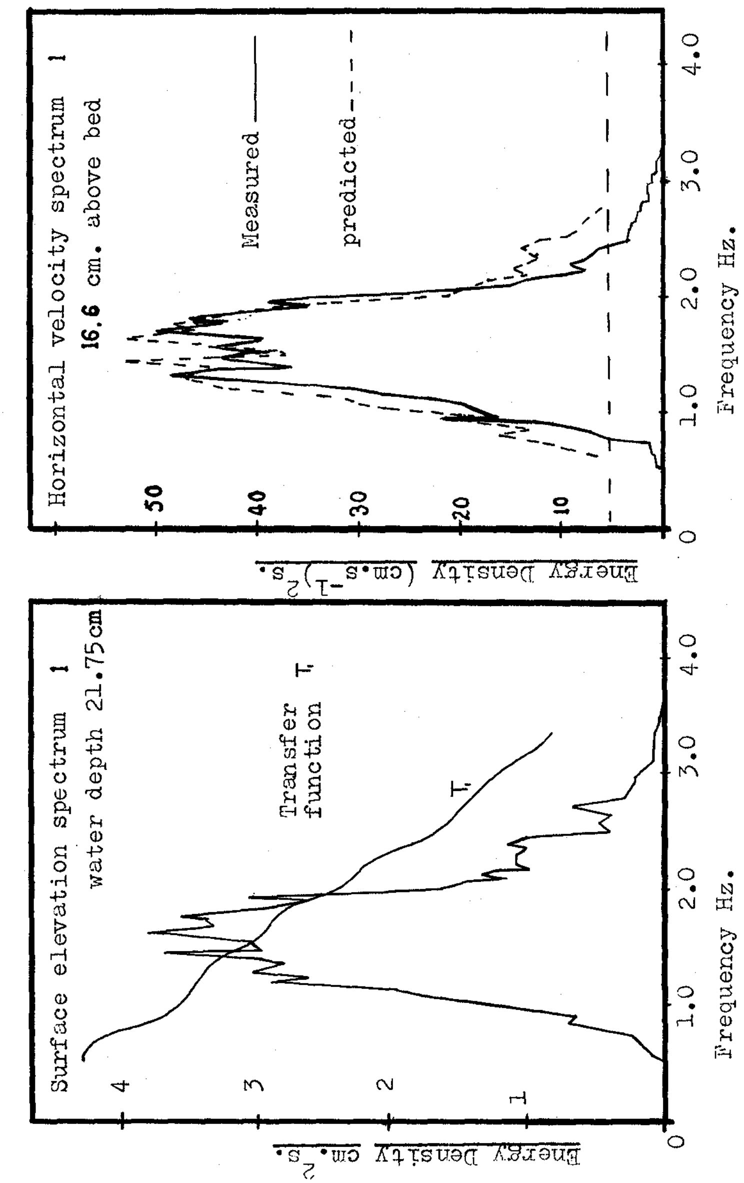
Horizontal velocity spectrum 1
16.6 cm. above bed
Measured
predicted
Energy Density (cm.s-1)2 s.
Frequency Hz.
Surface elevation spectrum 1
water depth 21.75cm
Transfer function T
T
Energy Density cm.2 s.
Frequency Hz.

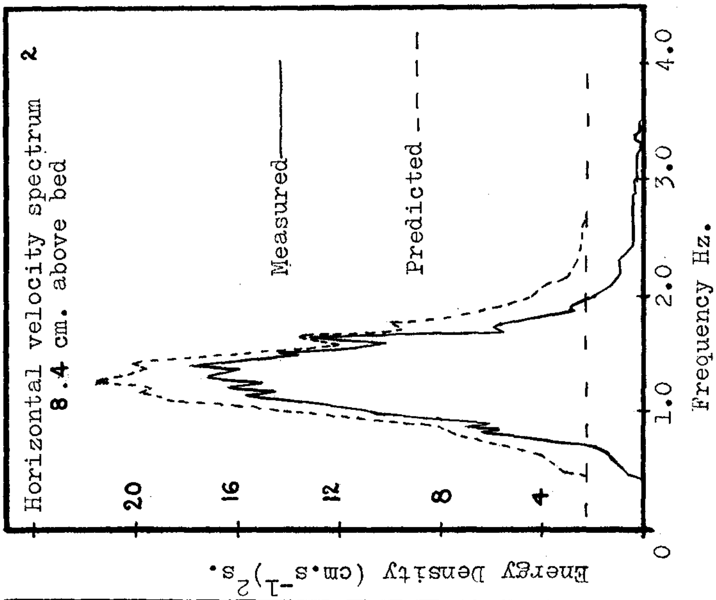
Horizontal velocity spectrum 2
8.4 cm. above bed
Measured
Predicted
Energy Density (cm.s⁻¹)²s.
Frequency Hz.
0
4
8
12
16
20
1.0
2.0
3.0
4.0

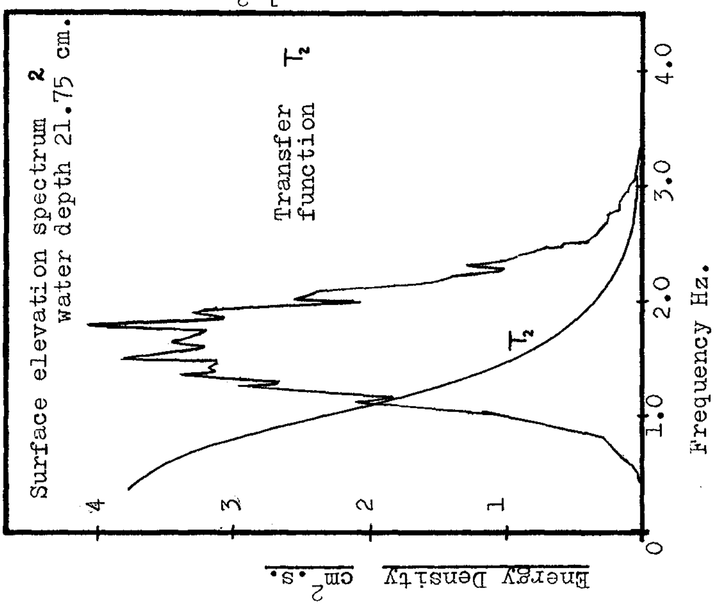
Surface elevation spectrum 2
water depth 21.75 cm.
Transfer function
T_2
Energy Density cm²s.
Frequency Hz.
0
1
2
3
4
1.0
2.0
3.0
4.0

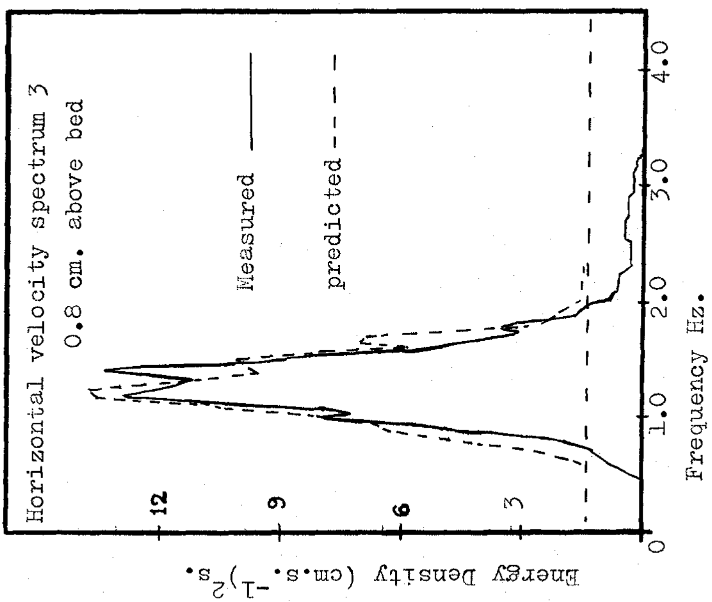
Horizontal velocity spectrum 3
0.8 cm. above bed
Measured
predicted
12
9
6
3
0
1.0
2.0
3.0
4.0
Frequency Hz.
Energy Density (cm.s.$^{-1}$)^{2}s.

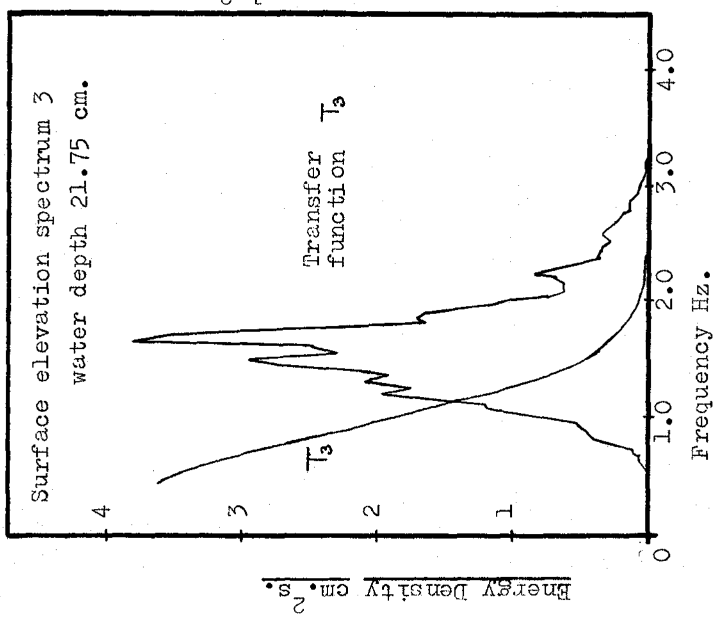
Surface elevation spectrum 3
water depth 21.75 cm.
Transfer function T_3
T_3
4
3
2
1
0
1.0
2.0
3.0
4.0
Frequency Hz.
Energy Density cm.^{2}s.